

# Biomimetic Synthesis of Pd Nanocatalysts for the Stille Coupling Reaction

Dennis B. Pacardo,<sup>†</sup> Manish Sethi,<sup>†</sup> Sharon E. Jones,<sup>‡</sup> Rajesh R. Naik,<sup>‡</sup> and Marc R. Knecht<sup>†,\*</sup>

<sup>†</sup>Department of Chemistry, University of Kentucky, 101 Chemistry-Physics Building, Lexington, Kentucky 40506-0055, and <sup>‡</sup>Nanostructured and Biological Materials Branch, Air Force Research Laboratory, Wright-Patterson Air Force Base, Ohio 45433-7702

**ABSTRACT** Here we report on the biomimetic synthesis of Pd nanoparticles for use as models of green catalytic systems. The nanomaterials are synthesized using peptides isolated *via* phage-display techniques that are specific to Pd surfaces. Using this synthetic strategy, peptide-functionalized Pd nanoparticles of  $1.9 \pm 0.3$  nm in diameter are produced, which are soluble and stable in aqueous solutions. Once characterized, these biobased materials were then used as catalysts to drive the formation of C–C bonds using the Stille coupling reaction. Under the conditions of an aqueous solvent at room temperature, quantitative product yields were achieved within 24.0 h employing catalyst loadings of  $\geq 0.005$  mol % of Pd. Additionally, high TOF values of  $3207 \pm 269$  mol product  $\cdot$  (mol Pd  $\cdot$  h)<sup>-1</sup> have been determined for these materials. The catalytic reactivity was then examined over a set of substrates with substitutions for both functional group and halide substituents, demonstrating that the peptide-based Pd nanoparticles are reactive toward a variety of functionalities. Taken together, these bioinspired materials represent unique model systems for catalytic studies to elucidate ecologically friendly reactive species and conditions.

**KEYWORDS:** peptides · Pd nanoparticles · catalysis · Stille coupling · bioinspired nanotechnology

The fabrication of green catalysts that address environmental and energy concerns is both strategically and ecologically important.<sup>1,2</sup> Traditional homogeneous and heterogeneous catalysts used on the industrial scale produce toxic waste materials that necessitate specialized disposal means and can require thermal activation for reactivity, both of which can result in inflated production costs. To alleviate these costly conditions, highly active green catalytic systems that employ an aqueous medium at room temperature with low catalyst loadings are desirable.<sup>3</sup> Metallic Pd nanoparticles have demonstrated some positive progression toward these goals;<sup>4–6</sup> however, it is rare for one system to address all three principles simultaneously. One further compounding issue is the fact that different catalyst structures can be required for their individual activity;<sup>7,8</sup> therefore, a “magic bullet” system that can be employed for all reactions is unlikely. As a result, different catalytic architectures may

be required for specific reactions, depending upon their structure-based functionality; however, a subset of reactions that follow similar pathways may be addressable by a single generated catalytic structure.

One area where a green reaction system is attractive is for catalytic C–C bond formation. A variety of reactions have been developed such as Stille coupling, Suzuki coupling, and Heck coupling that use Pd catalysts of similar morphologies.<sup>3–6,9</sup> These reactions traditionally employ single molecule Pd catalysts, either in the zerovalent state or in a Pd<sup>2+</sup> oxidation state that is reduced *in situ*, which require high thermal activation temperatures (70–100 °C) and organic solvents such as toluene.<sup>3,10</sup> Since similar mechanisms have been proposed for these reactions with only slight changes in specific steps, it may be possible to design and develop a single catalytic architecture that is functional for a select number of carbon coupling reactions using green conditions. This would be highly desirable as these reactions are used as necessitated by the functionalities and specific reaction steps required during chemical synthesis. Previous results employing Pd nanomaterials as the catalyst with different surface protection techniques have demonstrated a degree of success with these reactions individually.<sup>3–7,11–14</sup> Unfortunately, ideal materials that fully address the principles of green C–C coupling catalysis have yet to be isolated; however, development of systems to model and understand these processes is of interest to gain insight into the structural components required for reactivity.

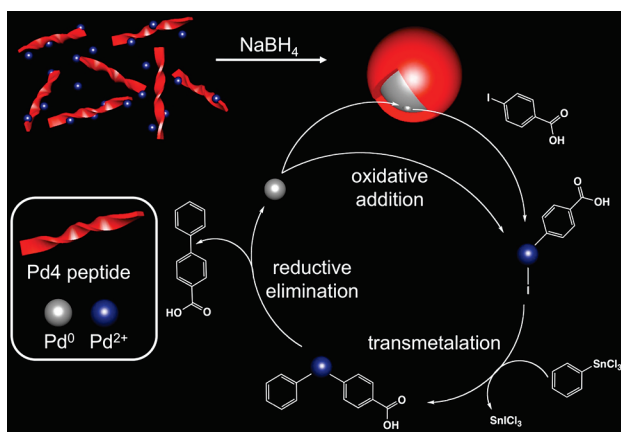
In contrast, biological systems have developed ambient synthetic routes to reactive nanostructures.<sup>16–19</sup> Through biomineralization processes,<sup>15,16</sup> highly intricate

\*Address correspondence to mrknech2@email.uky.edu.

Received for review March 18, 2009 and accepted April 21, 2009.

Published online May 7, 2009.  
10.1021/nn9002709 CCC: \$40.75

© 2009 American Chemical Society



**Scheme 1.** Biomimetic synthesis of Pd nanoparticles and their use for green Stille coupling.

nanomaterials can be produced for structural, catalytic, and bioremediation purposes. While a select number of inorganic minerals are fabricated biologically, a complete set of technologically interesting materials is not produced. To overcome this limitation, phage-display technologies have been developed as a means to expand the toolkit of bionanotechnology through the isolation of non-natural peptide sequences with the ability to control the fabrication of nanomaterials under biological conditions.<sup>17–23</sup> From this method, peptides responsible for the production of Ag,<sup>18</sup> Au,<sup>24</sup> FePt,<sup>23</sup> BaTiO<sub>3</sub>,<sup>21</sup> as well as other technologically interesting materials have been elucidated. The synthetic methodologies employed for biomimetic fabrications are relatively green and produce quality nanomaterials with exacting control over their final structural properties.<sup>20,25–28</sup> Indeed, multicomponent functional nanostructures have been fabricated such as PdAu bimetallic catalysts,<sup>25</sup> Pt–CdS enzyme mimics,<sup>27</sup> and Au–Co<sub>3</sub>O<sub>4</sub> biobatteries.<sup>20</sup> These unique structures possess their intrinsic activities under biological-based conditions, suggesting that their activities can be tailored to address green technologies. While these materials may not be immediately feasible to replace current methodologies, their final products can act as model systems to generate an understanding of the structure required for specific functionality. This may lead to the realization of next generation materials to address the current global environmental and energy concerns.

Here we demonstrate that peptides isolated *via* phage display are able to mediate the production of highly active model green Pd nanocatalysts, as shown in Scheme 1. Using the peptide-based system, nearly monodisperse and aqueously soluble peptide-stabilized Pd nanoparticles are synthesized with a small average particle diameter of  $1.9 \pm 0.3$  nm. This particle size is optimal for catalytic designs as it maximizes the surface-to-volume ratio without reaching the molecule to particle electronic transition of small nanomaterials.<sup>8</sup> These nearly monodisperse biobased nanoparticles were then catalytically tested for C–C bond formation activity using Stille coupling<sup>10,29</sup> under environmentally

friendly reaction conditions. From this analysis, quantitative catalytic formation of C–C bonds was observed within 24.0 h in water, at room temperature, using catalyst loadings of  $\geq 0.005$  mol % of Pd. These results are important as this representative system addresses all three green concerns, which is likely due to the peptide–metal surface structure that can allow for interactions between the catalytic surface and the reagents in solution.<sup>30</sup> In addition, we demonstrate that the bioinspired Pd materials are active with a variety of substrates, suggesting that the system is versatile and may translate to various other chemical reactions.

## RESULTS AND DISCUSSION

Pd-binding peptides were identified from a phage-displayed combinatorial peptide library. Commercially available Pd nanopowder (particle size <25 nm) was used as the target for identifying Pd-binding peptides from the peptide library using established procedures.<sup>17–19,21</sup> As shown in Table 1, two 12-mer sequences were identified, termed Pd2 and Pd4, respectively. Both peptide sequences possessed basic pI values; however, the Pd4 peptide sequence possessed more basic and hydroxyl-containing residues, comparatively. Additionally, theoretical modeling of the Pd4 peptide Pd surface binding capabilities suggests that the two histidine residues bind to the materials surface in a pinched arrangement, which will likely lead to open interaction sites between the solution and the metallic surface.<sup>30</sup> As such interactions are key to catalysis, this peptide was selected for nanoparticle synthetic analysis. The linear peptide was produced using standard Fmoc synthesis, purified by HPLC methods, and confirmed by MALDI-TOF mass spectrometry. Upon sequence confirmation, the peptide was then dissolved in deionized water to a concentration of 10 mg/mL, from which 100  $\mu$ L was added to a vial containing 25.0  $\mu$ L of 100 mM K<sub>2</sub>PdCl<sub>4</sub> in 4.775 mL of H<sub>2</sub>O. The solution was allowed to stand for 30.0 min, after which 100  $\mu$ L of a 100 mM NaBH<sub>4</sub> solution was added for metal reduction. Prior to reduction, the solution was a pale yellow color, owing to the PdCl<sub>4</sub><sup>2–</sup> in solution; however, after reductant addition, a rapid color change to brown was immediately observed. The solution was allowed to stand and reduce for 1.00 h prior to use.

Initial characterization was performed using UV–vis spectroscopy, as shown in Figure 1. The black spec-

**TABLE 1.** Pd Binding Peptide Sequences Identified Using Phage Display

peptide	amino acid sequence	pI <sup>a</sup>
Pd2	NFMSLPRLGMMH	9.8
Pd4	TSNAVHPTLRHL	9.5

<sup>a</sup>The pI was calculated at <http://ca.expasy.org>.

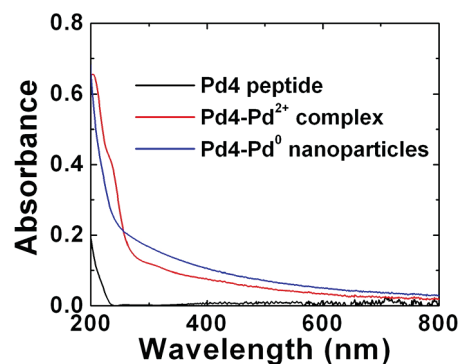


Figure 1. UV-vis spectra for the biomimetic synthesis of Pd nanoparticles. The black spectrum is for the Pd4 peptide, the red spectrum represents the Pd4-Pd<sup>2+</sup> complex, while the blue spectrum corresponds to the Pd nanoparticles after reduction. All spectra were background subtracted against water.

trum presented for the peptide in solution displays a featureless absorbance spectrum as anticipated. Upon incubation of the Pd4 peptide with the Pd<sup>2+</sup> ions (red spectrum of Figure 1), formation of an absorbance shoulder at 224 nm is observed. This absorbance is likely due to the ligand to metal charge transfer band associated with Pd-amine binding. The Pd4 peptide possesses histidine and arginine residues, which are readily able to coordinate Pd<sup>2+</sup> ions in solution to give rise to this spectral absorbance.<sup>31,32</sup> Upon reduction, represented by the blue spectrum, this band disappears with formation of a broad absorbance characteristic of nanoparticle formation.<sup>32,33</sup> An increase in absorbance toward lower wavelengths is observed for the reduced species, corresponding to the brown solution described above. Previous syntheses of small Pd nanoparticles have demonstrated similar colorimetric and UV-vis spectroscopic properties.<sup>8,34</sup> Additionally, no materials precipitation was observed at any point during the nanoparticle synthesis, suggesting that the interaction between the peptide and the nascent nanoparticle surface is sufficient in magnitude to prevent bulk material aggregation.

Transmission electron microscopy (TEM) confirmed the fabrication of nanoparticles, as displayed in Figure 2. Using this peptide, nearly monodisperse, spherical Pd nanoparticles are produced with an average diameter

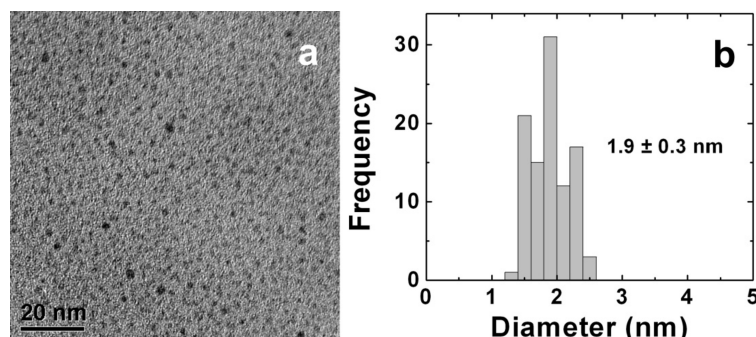


Figure 2. TEM analysis of the Pd nanoparticles. (a) TEM image of the Pd nanoparticles, and (b) size distribution histogram.

of  $1.9 \pm 0.3$  nm, which is highlighted in the particle size histogram presented in Figure 2b. On the basis of theoretical calculations assuming an empirical Pd atomic radius of 140 pm,<sup>35</sup> Pd nanoparticles of this size would contain approximately 312 metal atoms.<sup>36</sup> Such small particles are ideal for catalysis with their large surface-to-volume ratio for maximal catalytic activity. Additionally, the particles are large enough to avoid any undesired electronic effects that can be observed from smaller Pd nanostructures.<sup>8</sup>

To confirm that the synthetic protocol produced spherical Pd nanoparticles in response to the Pd4 peptide, rather than through generalized binding processes, control studies were conducted using a different peptide sequence of similar biological characteristics. In this analysis, the Pd4 peptide was substituted with the R5 peptide, which has been implicated in the biosilicification process of the diatom *Cylindrotheca fusiformis*.<sup>37,38</sup> Similar to the Pd4 peptide, the R5 peptide possesses a basic pI value (11.22) and a high percentage of basic and hydroxyl-terminated residues. Analysis of the materials prepared using this peptide resulted in the production of large, nonspherical Pd nanostructures of irregular networks, which are shown in the Supporting Information, Figure S1. No spherical particles were observed, and only wire-like structures were produced using the non-Pd-specific peptide. This dramatic change in shape and dispersity results in a minimization of the Pd surface area for interactions with the catalytic reagents, whereby decreasing their overall reactivity. This indicates that the Pd4 peptide possesses significant control over the fabrication of Pd nanomaterials, which can be synthetically preferred for the present catalytic applications.

Upon confirmation of the fabrication of Pd metallic nanostructures, the materials were studied for catalytic reactivity for the formation of C-C bonds. This family of reactions can follow various pathways; however, the overarching mechanism driving product generation is relatively similar from reaction to reaction. Initially, Stille coupling between an aryl halide and an organostannane compound was selected for analysis. This reaction was selected for three specific reasons. First, the final organic product of the catalytic reaction possesses a newly

formed C-C bond, which is important for pharmaceutical production,<sup>39</sup> molecular electronics,<sup>40</sup> and fossil fuel processing.<sup>41</sup> Second, previous reports have suggested that routes toward more environmentally responsible synthetic conditions for this carbon coupling scheme may be readily achievable.<sup>3</sup> Third, many of the reagents, both aryl halides and organostannanes, are commercially available to be used for facile characterization of the reactivity of the newly produced biomimetic Pd nanoparticles. Additionally, the solubility of the reagents can be tailored to fit a variety of solvent polarities and reaction conditions, thus facilitating a

broad set of analyses of the Pd nanomaterial's catalytic activity.

For catalytic analysis of the biomimetic materials, green synthetic conditions were initially employed for the coupling of 4-iodobenzoic acid and phenyltin trichloride to produce biphenyl carboxylic acid (BPCA), which was used as a model system.<sup>5</sup> For this reaction, 0.500 mmol of the aryl halide was codissolved in solution with 0.600 mmol of phenyltin trichloride using 8.00 mL of 2.25 M aqueous KOH. To this solution were added varying amounts of the Pd materials (0–0.500 mol % of Pd), and the reaction was stirred for 24.0 h. In this sense, the mol % of Pd refers to the amount of Pd in solution and not the concentration of nanoparticles, which would be quite lower. Once complete, the reaction was quenched with HCl, extracted using diethyl ether, and quantitated.

Initially, the model reaction was studied using 0.100 mol % of Pd. This concentration was used to determine the feasibility of the reaction under the described synthetic conditions employing the peptide-stabilized Pd nanoparticles. Visual monitoring of the solution during the reaction occurred from which the precipitation of a fine white solid within 10.0 min after initiation was observed. This event suggests that a successful catalytic reaction is progressing as the final product, BPCA, is not soluble in the hydrophilic solution. After reaction workup from which the organically soluble materials were extracted into diethyl ether, the final products were analyzed using GC–MS and <sup>1</sup>H NMR. For GC–MS analysis, the carboxylic acid containing species were converted into trimethyl silyl esters to prevent hydrogen bonding and increase the volatility for gas chromatographic analysis. Figure 3a presents the gas chromatogram of the reaction after functionalization. In this sample, 4-*tert*-butyl phenol (TBP) was added as an internal standard. The chromatogram possesses two distinct peaks at elution times of 7.29 and 11.04 min, which were analyzed by mass spectrometry in Figure 3b,c, respectively. Analysis of the materials from the 7.29 min peak (Figure 3b) indicates that it is the TBP internal standard, with an  $m/z = 222$ . The second peak observed at 11.04 min and analyzed in Figure 3c, possessed an  $m/z = 270$ , which is in agreement with the

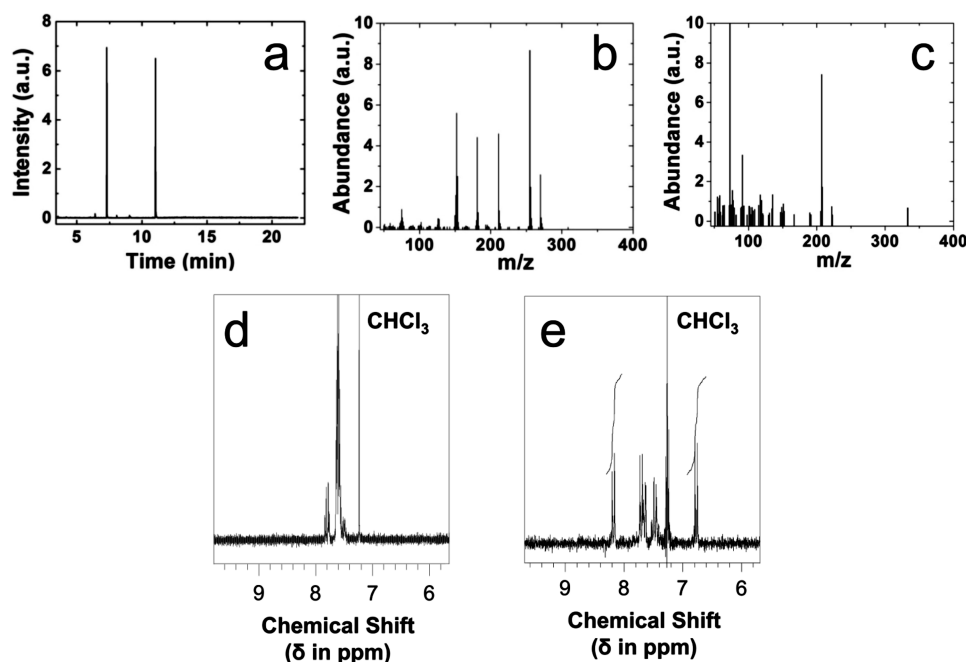


**Figure 3.** Characterization of the catalytic reaction between 4-iodobenzoic acid and phenyltin trichloride to produce BPCA. (a) Gas chromatogram for the final products after addition of the TBP internal standard. (b) Mass spectrum of the 7.29 min peak of the chromatogram. (c) Mass spectrum of the 11.04 min peak of the chromatogram. Analysis of each spectrum confirms that panel (b) represents the TBP internal standard, while panel (c) represents the anticipated silyl-functionalized BPCA final product. (d) NMR spectrum of the physical mixture of 4-iodobenzoic acid and phenyltin trichloride prior to catalyst addition and (e) NMR spectrum of the materials attained after catalytic reactivity with the bioinspired Pd nanoparticles. A new signal is observed at 8.2 ppm, consistent with the BPCA product.

calculated mass of the anticipated final BPCA product with the silyl-derivatized carboxylic acid. Additionally, no peak was isolated for the starting materials. While these results indicate a successful coupling reaction, spectroscopic characterization of the final product is required to confirm its identity.

Spectroscopic identification of the final materials was conducted using a 400 MHz <sup>1</sup>H NMR. Figure 3d presents the NMR spectrum of a mixture of the 4-iodobenzoic acid and phenyltin trichloride starting materials prior to catalysis initiation dissolved into a CDCl<sub>3</sub> solution. In this spectrum, peaks are observed at 7.78 and 7.87 ppm with a coupling constant of  $J = 8.8$  Hz. Such results are anticipated for the *para*-disubstituted benzene ring of the aryl halide substituent. The signals observed over the 7.5–7.7 ppm region are consistent with the known spectrum of the organostannane species.<sup>5</sup> Taken together, this indicates that only signals directly attributable to the starting materials are present, confirming that no reaction has taken place in the absence of the Pd nanoparticles. Analysis of the extracted products postreaction is shown in Figure 3e. This NMR spectrum demonstrates that the starting material peaks have disappeared and are replaced by a new signal at 8.17 ppm. Such clear results are consistent with the BPCA final product,<sup>5</sup> thus indicating that a successful catalytic carbon coupling reaction occurred in the presence of the bioinspired Pd nanomaterials. For this spectrum, an additional peak at 6.80



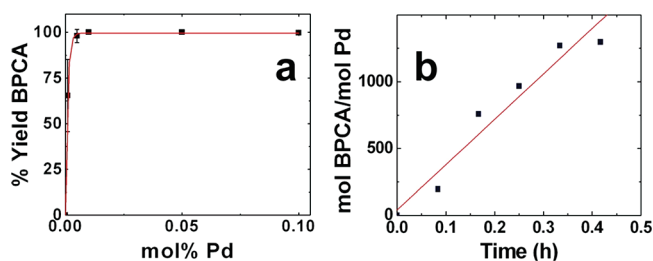


**Figure 4.** Analysis of the catalytic reactivity of the peptide-functionalized Pd nanoparticles. (a) Effect of Pd catalyst loading on the model reaction for the production of BPCA, and (b) TOF determination employing a catalyst loading of 0.050 mol % of Pd for the model reaction.

ppm is due to the TBP internal standard, whose individual spectrum was attained and is presented in the Supporting Information, Figure S2. The reaction was quantitated using the TBP, which indicates that a 100% product yield is attained within the 24.0 h reaction time frame.

To determine the extent of catalytic reactivity of the peptide-functionalized Pd nanoparticles, the model reaction was conducted at decreasing catalyst loading values. This process was studied down to a loading of 0.001 mol % of Pd with surprising product yields. As shown in Figure 4a, quantitative reaction yields were consistently achieved after a 24.0 h reaction time period down to a catalyst loading value of 0.005 mol % of Pd. Note that this percentage represents the amount of Pd atoms in solution, not the concentration of Pd nanoparticles; therefore, the loading value is even further minimized for the nanoparticle catalyst species. Remarkably, when a catalyst loading of 0.001 mol % was studied, an average product yield of ~64% was observed. While such catalyst loadings are below traditional values, these reactions were also conducted in an aqueous solvent at room temperature, suggesting that the bioinspired Pd nanomaterials may represent a model catalytic system for understanding the structural requirements of green catalysts. To confirm that the observed results were facilitated by the Pd nanoparticles rather than by an uncontrolled autocatalytic event, a control study was conducted in which no Pd nanoparticles were added to the two starting materials in a typical reaction solution. After 24.0 h, the sample was quenched and extracted using the standard purification and reaction procedures. Final analysis of the resultant materials indicated that no product was generated and that only the initial starting materials were retained.

To determine the efficiency of the peptide-functionalized Pd nanomaterials, the turnover frequency (TOF) of the reaction was determined. For this study, a Pd loading of 0.050 mol % was employed in a scaled up reaction volume of 80.0 mL. This system was used where the ratio of starting materials to catalyst remained constant to allow for additional time-based aliquot removal and analysis. Immediately after catalyst

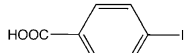
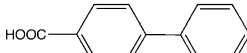
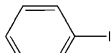
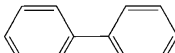
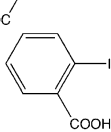
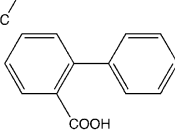
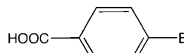
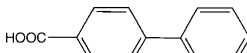
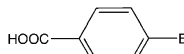
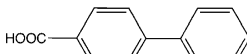
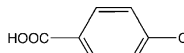
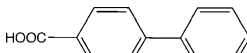
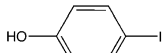
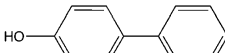
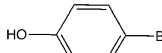
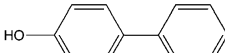
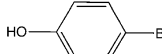
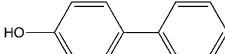
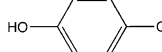
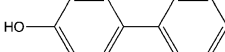
addition, one 8.00 mL aliquot was extracted from the reaction and quenched. From that time point, aliquots were taken and analyzed at 5.00 min intervals for 30.0 min and then at 10.0 min intervals for a total time of 1.00 h. The quantitation of the reaction yields at time points <30.0 min are plotted in Figure 4b, which represents the linear region of the analysis. The TOF value of this catalyst can then be extrapolated from the slope of the line over this portion of the plot as the y-axis incorporates both the mols of final product and catalyst. From this analysis, a TOF value of  $3207 \pm 269$  mol BPCA  $\cdot$  (mol Pd  $\cdot$  h) $^{-1}$  was determined for the model reaction system. This value is larger than those previously reported for similar systems and represents an enhancement in reactivity.<sup>4,5</sup>

An expanded analysis of the catalyst reactivity and specificity was further studied, as demonstrated in Table 2. For this analysis, the aryl halide was substituted at different positions and the halide functionality was varied over I, Br, and Cl substituents. Switching of the iodo substituent to the 3-position (entry 2) over the 4-position (entry 1) retained activity; however, when the iodo group was placed at the 2-position (entry 3), no product was generated. A lack of reactivity for this molecule was not unexpected due to irreversible binding to the Pd surface through the electronic interactions of the closely spaced functional groups.<sup>4–6</sup> Substitution of the halide for bromide or chloride functionalities resulted in a decrease in reactivity. Such results were anticipated due to the lesser activity of the lighter halides.<sup>10,29</sup> For the bromo species, when 0.100 mol % (entry 4) catalyst was used, a 7.9 or 43.2% yield was observed after 72 or 168 h of reactivity at room temperature, respectively. However, when 0.500 mol % (entry 5) catalyst was employed, an increased yield of 40.0 or 84.7% was attained after 72 or 168 h, respectively. Unfortunately, the 4-chlorobenzoic acid species (entry 6) was nonreactive toward carbon cross-coupling.

Further reactivity was probed using aryl phenols. Again, quantitative yields for the 4-iodo species (entry 7) were observed after 24.0 h. Substitution of the halide similarly resulted in decreased reaction yields; however, a significant product yield was still observed for the bromo species at either 0.100 mol % (entry 8) or 0.500 mol % (entry 9) catalyst after 72–168 h. The changes with this species, as compared to the carboxylic acid species, are likely due to the electronics of the molecule,<sup>10,29</sup> as well as catalyst concentration effects,<sup>12</sup> both of which are known to alter reactivity in solution. Overall, while varying yields can be achieved with differently substituted starting materials, final products are readily producible using green synthetic conditions catalyzed by the bioinspired Pd materials.

On the basis of the hydrophilic peptide coating of the biomimetic Pd nanoparticles, the system is likely to be optimized for aqueous-based reactivity. To probe this level of functionality, the model reaction using

TABLE 2. Stille Cross Coupling Reactions Using the Bioinspired Pd Nanoparticles<sup>a</sup>

Entry	Aryl Halide	Product	Yield
1			100
2			100
3			0
4 <sup>b</sup>			7.9 (43.2) <sup>c</sup>
5 <sup>d</sup>			40.0 (84.7) <sup>c</sup>
6 <sup>b</sup>			0
7			100
8 <sup>b</sup>			6.23 (26.8) <sup>c</sup>
9 <sup>d</sup>			12.8 (48.4) <sup>c</sup>
10 <sup>b</sup>			0

<sup>a</sup>Reaction conditions: 1.0 equiv of aryl halide, 1.2 equiv of PhSnCl<sub>3</sub>, 0.05 mol % of Pd, 8.0 mL of 2.25 M KOH, 25 °C, *t* = 24 h. <sup>b</sup>0.1 mol % of Pd nanoparticles. <sup>c</sup>*t* = 72 h or 168 h in parentheses. <sup>d</sup>0.5 mol % of Pd nanoparticles.

4-iodobenzoic acid was studied in a solvent mixture of 3:1 EtOH/H<sub>2</sub>O. This reaction system was required to achieve solubility of all the reagents and the peptide-functionalized nanocatalysts, while possessing the ability to be directly compared to the aqueous-based results to generate an understanding of solvent effects. Using these conditions with a catalyst loading of 0.050 mol % of Pd, at a reaction time of 24 h, a BPCA final product yield of only 44.9% was achieved (Supporting Information, Figure S16). This is significantly lower than the quantitative yields observed under aqueous conditions. These results are likely due to the solvent polarity, which can cause changes to the particle ligand surface, such as tighter ligand packing, to alter the specific interactions that drive the chemical reactions in solution.

The above catalytic results indicate that the inorganic metallic surface must be solvent exposed in some manner. If the surface was completely bound and passivated by the peptides, then specific reactivity would not be observed. Previous computational studies have suggested that the two histidine residues of the Pd4 peptide are responsible for the surface binding ability.<sup>30</sup> As such, it may be possible for the peptides to form a bidentate interaction, thus arranging in a spe-

cific fashion on the three-dimensional Pd nanoparticle surface. Due to steric and geometric constraints of the large peptide framework, it would be unlikely for the peptides to tightly pack on the small particle surface; therefore, pockets of exposed metallic regions are likely to exist. It is from these regions that the initial oxidative addition process can occur to drive the Stille coupling reaction. While it is known that the reaction does occur, it is difficult to determine whether this process is progressing at the surface of the particle, or whether Pd ions are chemically extracted from the nanomaterial and the reaction is driven by these liberated species in solution.<sup>3</sup> Future research on this mechanism is required and presently being conducted.

The catalytic reaction conditions demonstrated herein adhere to green synthetic conditions; however, the peptide synthesis required to achieve the directing ligands employs traditional synthetic organic mechanisms. While such routes are less than desirable, the main focus is to understand the materials structure of the peptide-functionalized Pd nanoparticles in an attempt to generate an image of the architectural requirements for enhanced green catalysts. As such, the peptide-functionalized Pd nanoparticles represent unique models to understand these structural proper-

ties as they possess inherently efficient and nearly green catalytic abilities. Based upon these principals, future biomimetic ligands may be produced in a more environmentally efficient manner to fabricate structured Pd nanoparticles with similar catalytic capabilities. In addition, further steps to enhance the green aspects of these catalytic particles can be achieved by using less harmful boron reagents in Suzuki coupling over the organotin species of Stille coupling. Further research is required; however, the initial steps toward this goal have been demonstrated.

## CONCLUSIONS

Herein we have demonstrated the use of peptides for the specific fabrication of highly active model green catalysts. These materials were synthesized using basic peptide sequences isolated *via* phage-display techniques with the ability to recognize and bind metallic Pd surfaces. Using standard reduction methods, small, monodisperse Pd nanoparticles are formed. These materials are reactive for Stille coupling employing the environmentally friendly conditions of a water-based solvent at room tem-

perature, using low Pd loadings of  $\geq 0.001$  mol % of Pd. Large TOF values have also been achieved using these materials, indicative of active catalysts. Additionally, these biomimetic Pd nanocatalysts have demonstrated reactivity across a set of chemical compounds, suggesting that their activity may be open to a variety of chemical reactions. This unique catalytic property is likely dependent upon the nanoparticle surface structure, which is directly controlled by the orientation and surface binding of the Pd<sub>4</sub> peptide. Theoretical calculations show that only the histidine residues of the peptide bind to the surface,<sup>30</sup> suggesting that a significant fraction of the surface Pd atoms are solvent exposed. While varying reaction yields were observed with chemically different starting materials, the main message is that the reaction efficiently progresses with a variety of species. The methods described represent only a fraction of those that can be employed while retaining environmentally friendly conditions. Small changes can be used for enhanced reactivity from the starting point described herein, which are presently being studied.

## METHODS

**Chemicals.** All Fmoc-protected amino acids used in peptide synthesis were purchased from Advanced ChemTech (Louisville, KY). NaBH<sub>4</sub> was purchased from EMD (Gibbstown, NJ), K<sub>2</sub>PdCl<sub>4</sub>, 2-iodobenzoic acid, 4-bromobenzoic acid, 4-iodophenol, and 4-*tert*-butylphenol were purchased from Sigma-Aldrich (Milwaukee, WI), and 4-iodobenzoic acid, 3-iodobenzoic acid, 4-chlorobenzoic acid, 4-bromophenol, and 4-chlorophenol were purchased from TCI America (Wellesley Hills, MA). Phenyltin trichloride, *N*-methyl-*N*-(trimethylsilyl)trifluoroacetamide (MSTFA), CCl<sub>3</sub>D, anhydrous Na<sub>2</sub>SO<sub>4</sub>, NaCl, and KOH were purchased from Fisher (Pittsburgh, PA). All reagents were used as received. Milli-Q water (18 mΩ · cm; Millipore, Bedford, MA) was used throughout.

**Peptide Synthesis.** The Pd<sub>4</sub> peptide was prepared using a Tetras peptide synthesizer (CreoSalus, Louisville, KY) employing standard Fmoc peptide synthesis protocols.

**Preparation of Pd Nanoparticles.** The Pd nanoparticles were prepared as follows: 100 μL of a 10.0 mg/mL Pd<sub>4</sub> peptide solution was added to a vial containing 25.0 μL of 100 mM K<sub>2</sub>PdCl<sub>4</sub> in 4.775 mL of H<sub>2</sub>O. The solution was completely mixed using a vortexer and allowed to stand for 30.0 min. The reaction was then reduced by adding 100 μL of a 0.100 M freshly prepared NaBH<sub>4</sub> solution. The reaction was then allowed to stand for 1.00 h at room temperature.

**Catalytic Reaction.** The coupling reaction of 4-iodobenzoic acid and phenyltin trichloride is presented as the model procedure in this analysis; however, identical protocols are used for all aryl halides employed. In 20.0 mL reaction vials, 124 mg (0.500 mmol) of 4-iodobenzoic acid and 98.6 μL (0.600 mmol) of phenyltin trichloride (PhSnCl<sub>3</sub>) were dissolved in 6.00 mL of 3.00 M aqueous KOH and 2.00 mL of H<sub>2</sub>O. Different amounts of Pd nanoparticle catalyst were then added to the reaction mixtures, namely, 1.00 mL (0.100 mol %), 0.500 mL (0.050 mol %), 100 μL (0.010 mol %), 50.0 μL (0.005 mol %), 10.0 μL (0.001 mol %), 5.00 μL (0.0005 mol %), and 1.00 μL (0.0001 mol %). The reactions were allowed to proceed for 24.0 h with constant stirring at room temperature. The reactions were then quenched with 50.0 mL of 5.00% aqueous HCl. The product of the reaction was extracted from the aqueous mixture using diethyl ether (thrice, 30.0 mL each). The organic layer was treated with saturated NaCl solution (twice, 20.0 mL each), dried with anhydrous Na<sub>2</sub>SO<sub>4</sub>, and fil-

tered; 75.0 mg (0.500 mmol) of 4-*tert*-butylphenol was added to the organic layer to serve as the internal standard in determining the percent yield of the reaction. The organic solvent was then removed using a rotary evaporator and the product was analyzed using GC-MS and <sup>1</sup>H NMR.

**TOF Measurement.** In determining the TOF of the catalyst, the reaction was monitored for 1.00 h at time intervals of 0.00, 5.00, 10.0, 15.0, 20.0, 25.0, 30.0, 40.0, 50.0, and 60.0 min. The coupling reaction between 4-iodobenzoic acid and phenyltin trichloride was scaled up by 10.0-fold, and 8.00 mL aliquots were obtained after each time interval. In a 250 mL beaker, 1.240 g of 4-iodobenzoic acid (5.00 mmol) and 986 μL of PhSnCl<sub>3</sub> (6.00 mmol) were dissolved in 60.0 mL of 3.00 M aqueous KOH and 20.0 mL of H<sub>2</sub>O. Then, 5.00 mL of the Pd nanoparticle catalyst (0.050 mol %) was added to the reaction mixture, and an 8.00 mL aliquot was immediately quenched with 50.0 mL of 5.00% aqueous HCl. Aliquots were then taken after the specified time intervals and extracted as described above.

**Characterization.** UV-vis spectra of the Pd nanoparticles were obtained on an Agilent 8453 UV-vis spectrometer using a 1.00 mm path length quartz cuvette (Starna). The spectra obtained were background subtracted against water. Electron microscopy images were obtained using a JEOL 2010F TEM operating at 200 keV with a point-to-point resolution of 0.19 nm. Samples were prepared on 400 mesh Cu grids coated with a thin layer of carbon (EM Sciences). The solution (5.00 μL) was pipetted onto the surface of the grid and allowed to dry in air.

GC-MS spectra of the products were obtained using an Agilent 6890N Network GC system with an Agilent 5973 Network Mass Selective Detector. Products possessing carboxylic acids and phenols were converted to their trimethyl silyl ester analogues prior to analysis. Approximately 3–6 mg of the product was added with 200 μL of *N*-methyl-*N*-(trimethylsilyl)trifluoroacetamide (MSTFA). The reaction was stirred for 2.00 h, which resulted in the complete dissolution of the product and formation of the trimethyl silyl ester. The reaction mixture was then diluted in CH<sub>2</sub>Cl<sub>2</sub> and analyzed by GC-MS.

NMR spectra were obtained using a Varian Inova 400 MHz NMR with a quadruply tuned switchable probe. The product (1.0–2.0 mg) was dissolved in 1.50 mL of deuterated chloroform in a standard 5.00 mm NMR tube (Wilmad). The integra-

tion of the peak at  $\delta$  8.2 ppm (product) was compared with the integration of the peak at  $\delta$  6.8 ppm (internal standard) to obtain the percent yield of the reaction.

**Acknowledgment.** Acknowledgment is made to the Donors of the American Chemical Society Petroleum Research Fund for partial support of this research (M.K.) and Air Force Office of Scientific Research (R.N.). Further support from the University of Kentucky is also acknowledged. We thank L. Jackson and Dr. B. C. Lynn for MALDI-TOF characterization of the synthesized peptides, and Dr. A. Jakhmola for the R5 analysis.

**Supporting Information Available:** TEM images of Pd materials produced using the R5 peptide, and complete NMR and GC-MS characterization. This material is available free of charge via the Internet at <http://pubs.acs.org>.

## REFERENCES AND NOTES

- Armor, J. N. Energy Efficiency and the Environment: Opportunities for Catalysis. *Appl. Catal., A* **2000**, *194*–195, 3–11.
- Centi, G.; Ciambelli, P.; Perathoner, S.; Russo, P. Environmental Catalysis: Trends and Outlooks. *Catal. Today* **2002**, *75*, 3–15.
- Astruc, D. Palladium Nanoparticles as Efficient Green Homogeneous and Heterogeneous Carbon–Carbon Coupling Precatalysts: A Unifying View. *Inorg. Chem.* **2007**, *47*, 1884–1894.
- Diallo, A. K.; Ornelas, C.; Salmon, L.; Aranzaes, J. R.; Astruc, D. “Homeopathic” Catalytic Activity and Atom-Leaching Mechanism in Miyaura–Suzuki Reactions under Ambient Conditions with Precise Dendrimer-Stabilized Pd Nanoparticles. *Angew. Chem., Int. Ed.* **2007**, *46*, 8644–8648.
- Garcia-Martinez, J. C.; Lezutekong, R.; Crooks, R. M. Dendrimer-Encapsulated Pd Nanoparticles as Aqueous, Room-Temperature Catalysts for the Stille Reaction. *J. Am. Chem. Soc.* **2005**, *127*, 5097–5103.
- Ornelas, C.; Ruiz, J.; Salmon, L.; Astruc, D. Sulphonated “Click” Dendrimer-Stabilized Palladium Nanoparticles as Highly Efficient Catalysts for Olefin Hydrogenation and Suzuki Coupling Reactions under Ambient Conditions in Aqueous Media. *Adv. Synth. Catal.* **2008**, *350*, 837–845.
- Narayanan, R.; El-Sayed, M. A. Catalysis with Transition Metal Nanoparticles in Colloidal Solution: Nanoparticles Shape Dependence and Stability. *J. Phys. Chem. B* **2005**, *109*, 12663–12676.
- Wilson, O. M.; Knecht, M. R.; Garcia-Martinez, J. C.; Crooks, R. M. The Effect of Pd Nanoparticle Size on the Catalytic Hydrogenation of Allyl Alcohol. *J. Am. Chem. Soc.* **2006**, *128*, 4510–4511.
- Crabtree, R. H. *The Organometallic Chemistry of the Transition Metals*; 3rd ed.; John Wiley & Sons: New York, 2001.
- Stille, J. K. The Palladium-Catalyzed Cross-Coupling Reactions of Organotin Reagents with Organic Electrophiles. *Angew. Chem., Int. Ed. Engl.* **1986**, *25*, 508–524.
- Karousis, N.; Tsotsou, G.-E.; Evangelista, F.; Rudolf, P.; Ragoussis, N.; Tagmatarchis, N. Carbon Nanotubes Decorated with Palladium Nanoparticles: Synthesis, Characterization, and Catalytic Activity. *J. Phys. Chem. C* **2008**, *112*, 13463–13469.
- Reetz, M. T.; de Vries, J. G. Ligand-Free Heck Reactions Using Low Pd-Loading. *Chem. Commun.* **2004**, 1559–1563.
- Srimani, D.; Sawoo, S.; Sarkar, A. Convenient Synthesis of Palladium Nanoparticles and Catalysis of Hiyama Coupling Reactions in Water. *Org. Lett.* **2007**, *9*, 3639–3642.
- Xu, S.; Yang, Q. Well-Dispersed Water-Soluble Pd Nanocrystals: Facile Reducing Synthesis and Application in Catalyzing Organic Reactions in Aqueous Media. *J. Phys. Chem. C* **2008**, *112*, 13419–13425.
- Dickerson, M. B.; Sandhage, K. H.; Naik, R. R. Protein- and Peptide-Directed Syntheses of Inorganic Materials. *Chem. Rev.* **2008**, *108*, 4935–4978.
- Slocik, J. M.; Knecht, M. R.; Wright, D. W. In *The Encyclopedia of Nanoscience and Nanotechnology*; Nalwa, H. S., Ed.; American Scientific Publishers: Stevenson Ranch, CA, 2004; pp 293–308.
- Dickerson, M. B.; Jones, S. E.; Cai, Y.; Ahmad, G.; Naik, R. R.; Kroger, N.; Sandhage, K. H. Identification and Design of Peptides for the Rapid, High-Yield Formation of Nanoparticulate TiO<sub>2</sub> from Aqueous Solutions at Room Temperature. *Chem. Mater.* **2008**, *20*, 1578–1584.
- Naik, R. R.; Stringer, S. J.; Argarwal, G.; Jones, S. E.; Stone, M. O. Biomimetic Synthesis and Patterning of Silver Nanoparticles. *Nat. Mater.* **2002**, *1*, 169–172.
- Lee, S.-W.; Mao, C.; Flynn, C. E.; Belcher, A. M. Ordering of Quantum Dots Using Genetically Engineered Viruses. *Science* **2002**, *296*, 892–895.
- Nam, K. T.; Kim, D.-W.; Yoo, P. J.; Chiang, C.-Y.; Meethong, N.; Hammond, P. T.; Chiang, Y.-M.; Belcher, A. M. Virus-Enabled Synthesis and Assembly of Nanowires for Lithium Ion Battery Electrodes. *Science* **2006**, *312*, 885–888.
- Ahmad, G. Rapid Bioenabled Formation of Ferroelectric BaTiO<sub>3</sub> at Room Temperature from an Aqueous Salt Solution at Near Neutral pH. *J. Am. Chem. Soc.* **2007**, *130*, 4–5.
- Sarikaya, M.; Tamerler, C.; Jen, A. K. Y.; Schulten, K.; Baneyx, F. Molecular Biomimetics: Nanotechnology through Biology. *Nat. Mater.* **2004**, *2*, 577–585.
- Reiss, B. D.; Mao, C.; Solis, D. J.; Ryan, K. S.; Thomson, T.; Belcher, A. M. Biological Routes to Metal Alloy Ferromagnetic Nanostructures. *Nano Lett.* **2004**, *4*, 1127–1132.
- Slocik, J. M.; Stone, M. O.; Naik, R. R. Synthesis of Gold Nanoparticles Using Multifunctional Peptides. *Small* **2005**, *1*, 1048–1052.
- Slocik, J. M.; Naik, R. R. Biologically Programmed Synthesis of Bimetallic Nanostructures. *Adv. Mater.* **2006**, *18*, 1988–1992.
- Slocik, J. M.; Zabinsky, S. I.; Phillips, D. M.; Naik, R. R. Colorimetric Response of Peptide-Functionalized Gold Nanoparticles to Metal Ions. *Small* **2008**, *4*, 548–551.
- Slocik, J. M.; Govorov, A. O.; Naik, R. R. Photoactivated Biotemplated Nanoparticles as an Enzyme Mimic. *Angew. Chem., Int. Ed.* **2008**, *120*, 5415–5419.
- Nam, K. T.; Lee, Y. J.; Krauland, E. M.; Kottmann, S. T.; Belcher, A. M. Peptide-Mediated Reduction of Silver Ions on Engineered Biological Scaffolds. *ACS Nano* **2008**, *2*, 1480–1486.
- Espinete, P.; Echavarren, A. M. The Mechanism of the Stille Reaction. *Angew. Chem., Int. Ed.* **2004**, *43*, 4704–4734.
- Pandey, R. B.; Heinz, H.; Farmer, B. L.; Slocik, J. M.; Naik, R. R.; Drummy, L. F. Adsorption of Peptides (A2, Flg, Pd2, Pd4) on Gold and Palladium Surfaces by a Coarse-Grained Monte Carlo Simulation. *Phys. Chem. Chem. Phys.* **2009**, *11*, 1989–2001.
- Slocik, J. M.; Moore, J. T.; Wright, D. W. Monoclonal Antibody Recognition of Histidine-Rich Peptide Encapsulated Nanoclusters. *Nano Lett.* **2002**, *2*, 169–173.
- Knecht, M. R.; Weir, M. G.; Frenkel, A. I.; Crooks, R. M. Structural Rearrangement of Bimetallic Alloy PdAu Nanoparticles within Dendrimer Templates to Yield Core/Shell Configurations. *Chem. Mater.* **2008**, *20*, 1019–1028.
- Creighton, J. A.; Eadon, D. G. Ultraviolet-visible Absorption Spectra of the Colloidal Metallic Elements. *J. Chem. Soc., Faraday Trans.* **1991**, *87*, 3881–3891.
- Scott, R. W. J.; Ye, H.; Henriquez, R. R.; Crooks, R. M. Synthesis, Characterization, and Stability of Dendrimer-Encapsulated Palladium Nanoparticles. *Chem. Mater.* **2003**, *15*, 3873–3878.
- [http://www.webelements.com/palladium/atom\\_sizes.html](http://www.webelements.com/palladium/atom_sizes.html), accessed February 25, 2009.
- Kim, Y.-G.; Oh, S.-K.; Crooks, R. M. Preparation and Characterization of 1–2 nm Dendrimer-Encapsulated Gold Nanoparticles Having Very Narrow Size Distributions. *Chem. Mater.* **2004**, *16*, 167–172.
- Knecht, M. R.; Wright, D. W. Functional Analysis of the Biomimetic Silica Precipitating Activity of the R5 Peptide



- from *Cylindrotheca fusiformis*. *Chem. Commun.* **2003**, *24*, 3038–3039.
38. Kröger, N.; Deutzmann, R.; Sumper, M. Polycationic Peptides from Diatom Biosilica that Direct Silica Nanosphere Formation. *Science* **1999**, *286*, 1129–1132.
  39. Nicolaou, K. C.; Bulger, P. G.; Sarlah, D. Palladium-Catalyzed Cross-Coupling Reactions in Total Synthesis. *Angew. Chem., Int. Ed.* **2005**, *44*, 4442–4489.
  40. Anthony, J. E. The Larger Acenes: Versatile Organic Semiconductors. *Angew. Chem., Int. Ed.* **2008**, *47*, 452–483.
  41. U.S. Department of Energy, Basic Research Needs: Catalysis for Energy, 2007.